A novel Franchot engine design based on the balanced compounding method

A novel Franchot engine design based on the balanced compounding method

Jafar M. Daoud, Daniel Friedrich*

School of Engineering, Institute for Energy Systems, University of Edinburgh, EH9 3DW (Scotland)

**Corresponding author Email: d.friedrich@ed.ac.uk*

Abstract: *The Franchot engine is a double acting Stirling engine with only two cylinders and freely controllable phase angle. The hot and cold cylinders of the Franchot engine can be directly heated and cooled and thus act as heaters/coolers. However, the cylinders are necessarily long and thin to increase the heat transfer area and hence the power. The long strokes result in long cranks and connecting rods which lead to large and unwieldy engines. In this contribution, the directly heated and cooled multi-cylinder Franchot engine is dynamically studied with a novel balanced compounding mechanism. Thus, the balanced compound Franchot engine would be more compact, cheaper and more efficient due to the removal of the rotational parts. The new mechanism includes a linkage between two connecting rods in a conventional Franchot engine for which, four pistons (an expansion, compression and two guiding pistons) move as one reciprocator. The influence of different engine parameters, such as number of cylinders, temperature, dead volume and reciprocator mass, on the new configuration is investigated. The possible phase angles for each number of cylinders are given. The balanced compound Franchot engine changes the order of piston motion so that the largest of these phase angles is obtained. The theoretical analysis shows that increasing the number of cylinders, dead volume and reciprocating mass reduces the frequency and increases the stroke; increasing the cylinder diameter increases the frequency and decreases the stroke; increasing the load decreases the stroke and slightly decreases the frequency; and increasing the temperature increases both the frequency and the stroke. Thus, different engine parameters can be used to maximise the power generation without the piston hitting the cylinder head. The dynamic load, which is a function of the speed, does not prevent the balanced compound Franchot engine from self-starting while static friction can prevent the engine from self-starting, especially if the pistons are around the mid-stroke point. The most promising configuration is the three-phase engine which has the lowest number of cylinders, preferable phase angle and phase shift of 120^o and potential for electricity generation and heat pumping.*

Keywords: *Franchot engine; Stirling engine; multi-cylinder; phase angle; phase shift; balanced compounding*

1 Introduction

The Franchot engine which is a double acting Stirling engine was invented in the 19th century by Charles Louis Franchot [1]. The design of Stirling engines, which is a compromise between power and thermal efficiency, is still an open and widely studied problem [2][3][4]. In the Franchot engine, only two pistons are required, the phase angle can be freely controlled and each cylinder is either hot or cold which eliminates the shuttle and axial conduction losses [5]. Double acting as well as single acting Stirling engines can use the simple slider crank drive [6][7]. Kinematic drives convert the reciprocal motion into rotational motion and mechanically fix the relation between engine parameters, such as the phase angle, phase shift and stroke length. However, kinematic Stirling engines were not cost effective, mechanically reliable or mass produced [8][9]. The free piston concept offers a linear driving mechanism without a need for a rotational cranking mechanism. The free piston concept can be used in applications for which the linear motion can be directly used, e.g. linear electricity generator, liquid pump, gas compressor or heat pump [10].

The free piston Stirling engine (FPSE) was introduced by Beale in 1969 and patented in 1972 for single acting engines which have the crankshaft replaced by gas or mechanical springs [11][12]. The force that is needed to complete the compression stroke is stored in the spring instead of being transferred through the crankshaft. The absence of the crankshaft results in the removal of the rotating parts, lubrication system, support structure and connecting rods. This implies that the FPSE has small side

thrust forces, excellent thermal efficiency, reduced mechanical wear and can be hermetically sealed which makes it compacter, more reliable and cheaper than conventional engines [11]. However, the FPSE experiences variations of the stroke length and phase angle as a response to the load and has hysteresis losses due to the internal friction of the springs which is dissipated as heat [8][13][14]. The FPSE might experience over strokes that cause the power piston to strike the cylinder ends [15][16]. Hence, auxiliary devices are needed to limit the stroke. The free piston concept can be extended to the multi-cylinder Siemens configuration where higher power density and a lower number of moving parts and springs are obtained. The reliability of the multi-cylinder FPSE can be increased if the pistons are replaced by membranes hence, mechanical friction can be avoided and sealing becomes much easier [9].

It has been reported that, at least three cylinders are needed to achieve the multi-cylinder Siemens engine [7][9][17]. Unlike the single acting engine where the phase angle is a function of spring stiffness, the multi-cylinder engine has its phase angle and phase shift governed by the number of cylinders. For each cylinder thermodynamically connected to an adjacent cylinder, the phase angle which defines the lag between hot and cold spaces can be represented as a function of the number N of cylinder as $\theta = 180^{\circ} - \frac{360^{\circ}}{N}$ [18]. The phase shift which determines the sequence of the reciprocating pistons is given by $\theta_S = \frac{360^{\circ}}{N}$ [19].

For any Stirling machine the preferred phase shift is within the range 90°-140° [20]. Only the three and four cylinder Siemens configurations fall into this range. At the highly preferable phase shift 120° which can be obtained from the 3 cylinder engine, a non-recommended phase angle equal to 60° is obtained which increases the fractional volumetric variation hence contributes in increasing the hysteresis losses [21].

A liquid piston engine (also known as Fluidyne) was invented by Colin D. West in 1969 [22]. In liquid piston engines, the mechanical pistons and connecting rods are replaced by liquid columns and the coupling forces in the FPSE are replaced by the hydrodynamic and hydrostatic forces [23]. In multi-cylinder liquid piston engines such as the Siemens configuration, each hot to cold space shares the same liquid column so that they are coupled pneumatically and hydraulically which defines the phase angle.

In 1978, Finkelstein [24] presented a novel coupling mechanism called the balanced compounding of Stirling machines for which he was granted a patent in 1980 [25]. Instead of storing some of the expansion energy in a rotating crankshaft, springs or hydrostatic columns for the compression stroke, an opposite engine group is added. Both engine groups are coupled mechanically through straight connecting rods. Thus, in this arrangement each connecting rod connects two cylinders. Hence, an even number of double acting Stirling machines is required. In the Finkelstein configuration, the connecting rods are located to the cold cylinder side and can be as short as possible due to the absence of heat transfer between the facing parts. By rearranging the engine compartment, a balanced compound 4 cylinder engine where each cylinder is either hot or cold can be obtained. This becomes a dual Franchot engine which eliminates heat conduction and shuttle losses but has heat transfer losses due to the connecting rod. In this configuration, the Franchot engines generate opposite forces as it comprise two opposite alpha type Stirling engine. Hot spaces are both gas and mechanically coupled to the cold spaces by the regenerators and connecting rods, respectively. However, to keep the phase angle advanced by 90° for all of the four hot spaces, half the regenerator connections are longer and have to cross.

Finkelstein showed in his patent many variations of the FPSE based on the balanced compounding technique. For example, a one-cylinder engine in which different work volumes are coupled mechanically using two concentric shafts can be equivalent to the 4-cylinder engine. Similar to the FPSE, this mechanism comprise the lowest possible side forces, absence of rotating parts, hence, increased seal life, improved engine performance and ability to hermitically seal engine compartments.

The balanced compound engine was investigated based on the phasor diagram and ideal Schmidt analysis of the isothermal Stirling engine [24]. The analysis shows that the proposed engine can generate net positive power. Finkelstein [26] obtained an analytical solution for the balanced compounding Vuilleumier cycle with two hot, two warm and two cold cylinders which require 8 regenerators with long connections, six hot heat exchangers and two connecting rods. His model is based on ideal assumptions, isothermal expansion and compression processes and only works with FPSE. The analytical solution showed that the piston oscillation is sinusoidal and the phase shift is 90^{o}. In 1992, Finkelstein [27] analysed the balanced compound Vuilleumier heat pump using a simpler model based on the sinusoidal variations of the swept volumes. The new model showed negligible differences with the FPSE model. The new model can be used for both the kinematic and free piston machines. However, no experimental study or real machine was reported to be manufactured.

McConaghy [28] patented a new arrangement for 3-phase AC power generation which is composed from two 3-ph gamma type engines working opposite to each other and coupled electrically. Each cylinder has a piston and a displacer rigidly coupled by a rod. This design makes it possible to get rid of the connecting rods between different cylinders and to hermetically seal all engine compartments but it still has a bounce volume, displacers and double the number of sliding objects. In addition to that, the operation is dependent on the load. In 2014, Dadd [29] patented a linear multi-cylinder Stirling machine. In this machine, the hot and cold volumes are coupled by gas and common connecting rods. This machine has the same number of connecting rods and cylinders but uses the linear power transmitters such as linear motors and generators as coupling mechanism.

In our previous work [30][31], we introduced, modelled and investigated the cylinder heated and cooled Franchot engine and developed a novel isothermaliser design to improve the power density. However, the engine still uses long cylinders to enhance the heat transfer and power generation. Long cylinders require long cranks which leads to a long engine, piston side forces and vibrations. A multi-cylinder configuration can enhance power generation and reduce the vibrations for the simple slider crank mechanism [32]. Nevertheless, rotational parts are responsible for increasing the complexity, unreliability, losses and cost. The use of gas or mechanical spring coupling might not be the suitable option for the cylinder heated and cooled engine. Long bounce spaces or long mechanical springs can generate large losses in addition to increasing the engine length. The directly heated and cooled Franchot engine cannot also use the balanced compounding innovated by Finkelstein due to long regenerator connections. Moreover, the opposite engines configuration requires only an even pair of hot cylinders and results in distributed heaters and coolers.

In this study, the slider crank mechanism is replaced by a novel driving method based on the balanced compounding principle. We extend our previous works to evaluate the impact of using the balanced compounding principle on the mechanical engine performance. In addition to the potential power improvements, this study investigates the potential of the engine to self-start. A tailored mathematical model for the balanced compound Franchot engine is derived which is suitable for an arbitrary number of cylinders.

2 Balanced compounding of the cylinder heated/cooled Franchot engine

Here, the side-by-side balanced compound arrangement is suggested which has reduced regenerator connection lengths and directly cooled and heated cylinders. It requires a minimum of three phases to make a multiple Franchot engine with straight and short regenerator connections. The top and side view for the balanced compound directly heated and cooled $n-ph$ engine are shown in Figure 1. Each cold cylinder is coupled with a conjugate hot cylinder mechanically via an external crank and through the regenerator to the corresponding hot cylinder of the engine. Each crank connects two Franchot engines and each Franchot engine is connected to two cranks according to the ordering shown. Only one long but straight regenerator connection is needed in the engine En which can be shorten by a round topology. Each compression piston can move parallel to an expansion piston at a predefined phase angle. The compression work will be compensated by the expansion work without a crankshaft and flywheel [24]. However, the zero side forces obtained by the Finkelstein arrangement are not achievable by this configuration. The side forces in this arrangement are expected to be smaller than the forces of the slider crank engine due to the shorter crank length. The crank length in the kinematic engine is half of the stroke length while the crank length in the balanced compound engine can be much shorter based on the required distance between the cylinders such as the need to add thermal insulators or mountings.

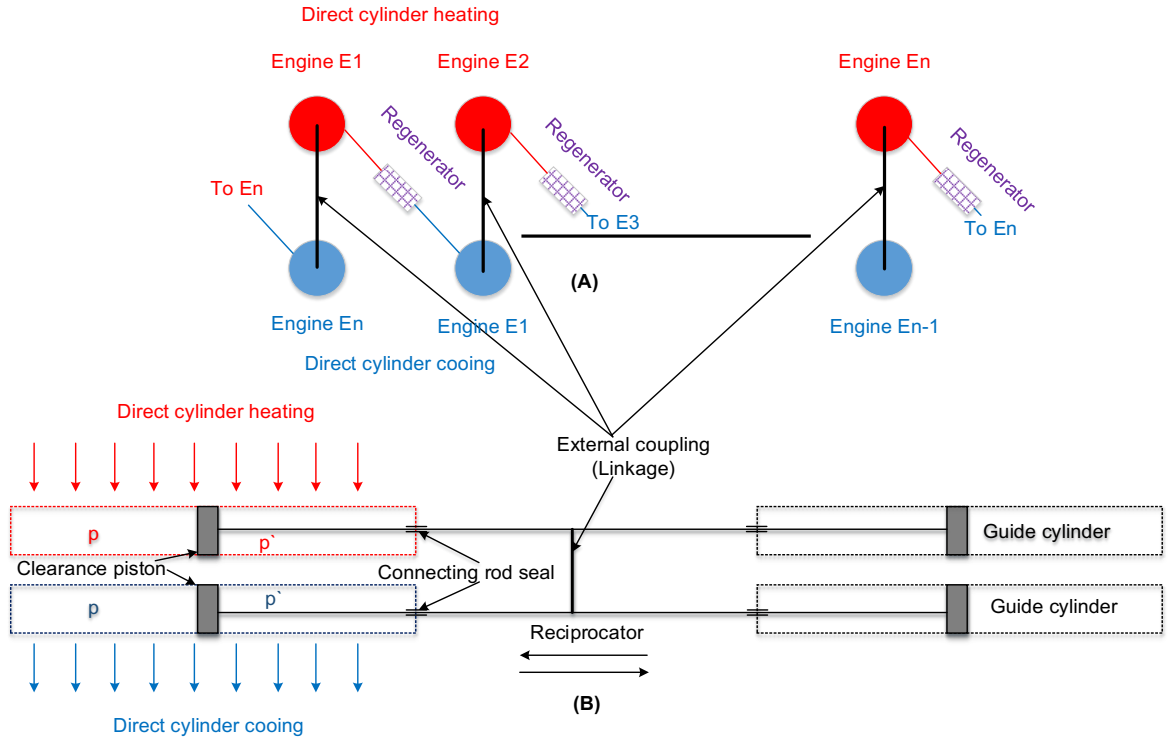

Figure 1: Balanced compounding of the multi-cylinder Franchot engine. A) cross sectional view showing the n-phase engine and B) side view showing two cylinders of the multi-cylinder configuration.

In the kinematic engine, the phase angle of the multi-cylinder Franchot engine can be predicted based on the regenerator connection as shown in Table 1 [32][33]. In the balanced compounding, the regenerator connection is determined by the order of piston motion. It is expected that the balanced compound engine will work on one of the listed angles. However, Berchowitz and Kwon [20] anticipated the phase angle will decrease for increasing the number of cylinders of the stepped piston design.

Table 1: Possible phase angles of the multi-cylinder Franchot engine for different numbers of cylinders

	3-ph	*4-ph*	*5-ph*	*6-ph*	*7-ph*	*8-ph*
y=2	120^o	90^o	72^o	60^o	51.4^o	45^o
y=4			144^o	120^o	102.8^o	90^o
y=6					154.2^o	135^o

Figure 2 shows the thermodynamic cycle of a Stirling engine having two opposite pistons. The expansion piston always leads the compression piston by an arbitrary phase angle. The direct cylinder heated and cooled Stirling engine comprises two polytropic and two isochoric processes according to piston motion from 1`-4`. The ideal engine has isothermal instead of the polytropic processes for the piston motion from 1-4, though.

- 1`-2` Polytropic compression: In this process, the expansion piston stands still and the compression piston moves inward. The heat is rejected alongside the walls of the cold cylinder corresponding to the working space due to the gas temperature difference with the cold cylinder walls. The engine requires some work in order to compress the working fluid and the pressure increases.
- 2`-3` Isochoric heating: In this process, the expansion and compression pistons move outward and inward, respectively. They move against each other and keep the total volume of the working spaces constant. The gas flows from the compression to the expansion space and passes through the regenerator which absorbs heat from it. In this process, the pressure of the gas increases and no work is required or generated since there is no change in the total engine volume.
- 3`-4` Polytropic expansion: In this process, the compression piston stands still and the expansion piston moves outward. Energy is absorbed alongside the wall of the hot cylinder corresponding to the hot working space due to the temperature difference between the hot cylinder walls and working gas. The cycle generates positive work and the gas pressure decreases.
- 4`-1` Isochoric cooling: In this process, the expansion piston moves inward and the compression piston moves outward . Both move against each other keeping the total volume of the working spaces constant. The gas flows from the expansion to the compression space through the regenerator. The gas re-absorbs the heat which was absorbed in step 2`-3` into the regenerator. In this process, no mechanical work is required or generated since there is no change in the total engine volume and the working gas pressure decreases.

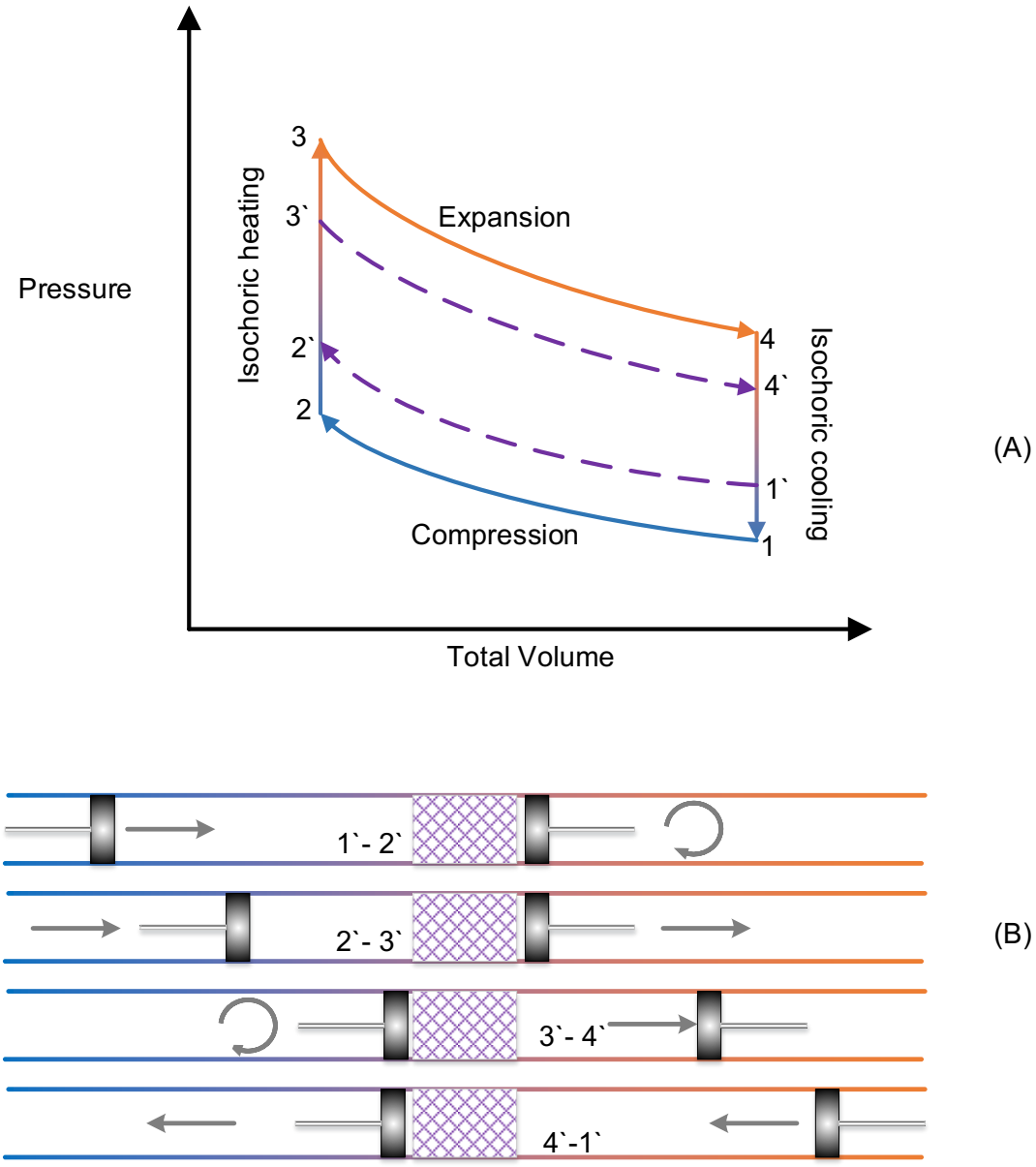

Figure 2: Thermodynamic cycle of the Stirling engine: A) PV diagram of the ideal (1-2-3-4) and polytropic (1'-2'-3'-4') cycle and B) piston displacements for the polytropic cycle.

3 Methodology

Figure 3 shows the relationship between the forces, reciprocators and displacement of each component of the balanced $n - ph$ Franchot engine. The $n - ph$ Franchot engine is composed from $2 * n$ alpha type Stirling engines. In which, each alpha type Stirling engine is modelled separately.

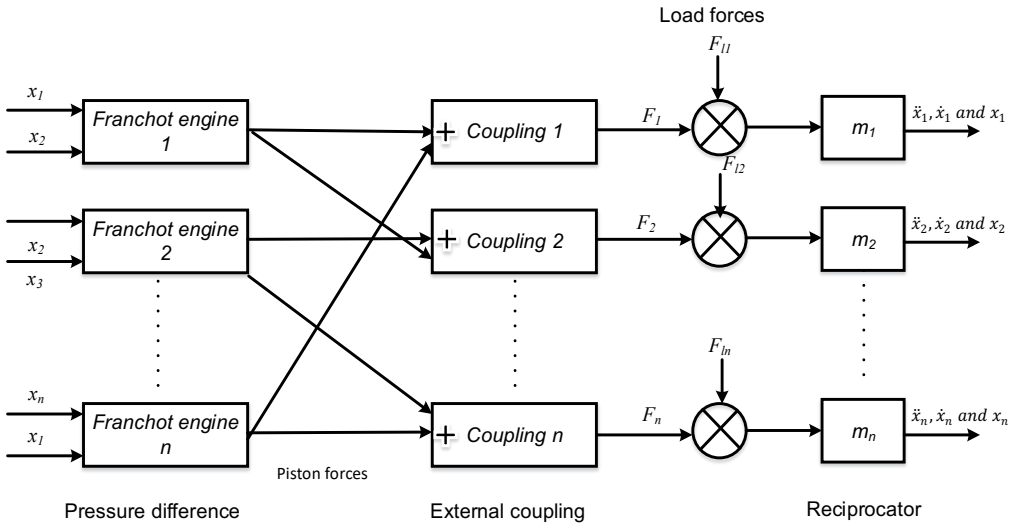

Figure 3: Schematic diagram of the $n-ph$ balanced compound Franchot engine which shows the forces and nomenclature.

Applying Newton's second law of motion, the force balance equation implies

$$\begin{bmatrix} F_1 \\ F_2 \\ \vdots \\ F_n \end{bmatrix} = \begin{bmatrix} m_1 \\ m_2 \\ \vdots \\ m_n \end{bmatrix} [\ddot{x}_1 \quad \ddot{x}_2 \quad \dots \quad \ddot{x}_n] + \begin{bmatrix} F_{l1} \\ F_{l2} \\ \vdots \\ F_{ln} \end{bmatrix} \qquad 1$$

where F is the thermal driving force, m is the total mass of reciprocating elements as a bulk, F_l is the load force, x is the reciprocator displacement.

The power is calculated for the $n-ph$ Franchot engine as follows

$$P = F_1\dot{x}_1 + F_2\dot{x}_2 + \cdots + F_n\dot{x}_n \qquad 2$$

The thermal forces applied to each connecting rod are calculated from

$$\begin{bmatrix} F_1 \\ F_2 \\ \vdots \\ F_n \end{bmatrix} = \begin{bmatrix} \Delta p_{E1} & \Delta p_{En} \\ \Delta p_{E2} & \Delta p_{E1} \\ \vdots & \vdots \\ \Delta p_{En} & \Delta p_{En-1} \end{bmatrix} \begin{bmatrix} A_{h1} & A_{h2} & \cdots & A_{hn} \\ A_{kn} & A_{k1} & \cdots & A_{kn-1} \end{bmatrix} \qquad 3$$

where $A_h \; and \; A_k$ are the cross sectional area of the hot and cold pistons respectively, Δp is the pressure difference across the pistons of the Franchot engine, F_l is the force due to the load and the subscript E denotes the Franchot engine.

If all reciprocators have the same cross sectional area and mass then the acceleration of the pistons can be calculated by rearranging the fore balance equation and the thermal forces to get the following equation:

$$\begin{bmatrix} \ddot{x}_1 \\ \ddot{x}_2 \\ \vdots \\ \ddot{x}_n \end{bmatrix} = \frac{A}{m} \left(\begin{bmatrix} \Delta p_{E1} + \Delta p_{En} \\ \Delta p_{E2} + \Delta p_{E1} \\ \vdots \\ \Delta p_{En} + \Delta p_{En-1} \end{bmatrix} - \begin{bmatrix} F_{l1} \\ F_{l2} \\ \vdots \\ F_{ln} \end{bmatrix} \right) \qquad 4$$

The speed and displacement of the pistons are calculated by calculating the integral and double integral of the acceleration matrix, respectively.

The free piston Stirling engine is considered a mass damper system where the generic load acting on its moving pistons can be approximated by a damping load in which the load force is written as [10][13][34][35]:

$$\begin{bmatrix} F_{l1} \\ F_{l2} \\ \vdots \\ F_{ln} \end{bmatrix} = \begin{bmatrix} c_1 \\ c_2 \\ \vdots \\ c_n \end{bmatrix} [\dot{x}_1 \quad \dot{x}_2 \quad \dots \quad \dot{x}_n] \tag{5}$$

where c is the damping coefficient.

The friction is another type of load that reduces the Stirling engine performance and needs to be reduced. For sliding pistons the coefficient of friction is around 0.2 [36]. There are two mechanical friction sources in this configuration; the friction due to the weight of the reciprocating masses and the friction due to the side forces created by the cylinder offset. The side forces can be obtained by analysing the free body diagram of the engine as shown in Figure 4. The analysis considers the worst case when the rod sleeves are tight enough to handle all mechanical friction. Besides their roll to guide the connecting rods, guiding cylinders can be used as additional engine to serve as a load like heat pump or fluid pump.

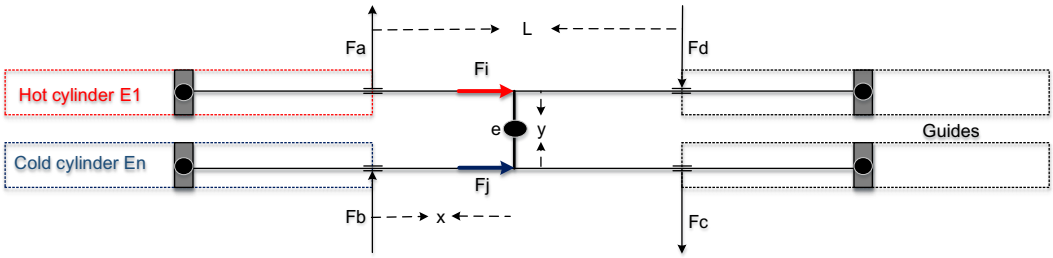

Figure 4: Free body diagram of the balanced compound Franchot engine.

Taking the moment of inertia around the non-rotating point e applies:

$$\sum M_e = 0 \tag{6}$$

hence,

$$\frac{y}{2}(F_j - F_i) - x(F_a + F_b) - (L - x)(F_c + F_d) = 0 \tag{7}$$

As the connecting rod is only free to move along the cylinder axis (x) then

$$\sum F_y = 0 \tag{8}$$

This implies that

$$F_a + F_b = F_c + F_d \tag{9}$$

hence, the total side force can be calculated as:

$$F_a + F_b + F_c + F_d = \frac{y * (F_j - F_i)}{L} = \frac{y}{L}\Delta F \tag{10}$$

where,

$$\Delta F = \begin{bmatrix} \Delta F_1 \\ \Delta F_2 \\ \vdots \\ \Delta F_n \end{bmatrix} = A \begin{bmatrix} \Delta p_{En} - \Delta p_{E1} \\ \Delta p_{E1} - \Delta p_{E2} \\ \vdots \\ \Delta p_{En-1} - \Delta p_{En} \end{bmatrix} \quad (11)$$

The load force due to the mechanical friction can be written as:

$$\begin{bmatrix} F_{l1} \\ F_{l2} \\ \vdots \\ F_{ln} \end{bmatrix} = \begin{bmatrix} \begin{cases} 0.2(m_1 g + |\Delta F_1|) & \dot{x}_1 < 0 \\ -0.2(m_1 g + |\Delta F_1|) & \dot{x}_1 > 0 \end{cases} \\ \begin{cases} 0.2(m_2 g + |\Delta F_2|) & \dot{x}_2 < 0 \\ -0.2(m_2 g + |\Delta F_2|) & \dot{x}_2 > 0 \end{cases} \\ \vdots \\ \begin{cases} 0.2(m_n g + |\Delta F_n|) & \dot{x}_n < 0 \\ -0.2(m_n g + |\Delta F_n|) & \dot{x}_n > 0 \end{cases} \end{bmatrix} \quad (12)$$

The resonant frequency of the free piston Stirling engine is a function of the reciprocating mass and spring stiffness as [37][19]:

$$\omega_o = \sqrt{\frac{k}{m}} \quad (13)$$

The spring stiffness of the balanced compound Franchot engine which is pressure coupled can be calculated from the stiffness of the working gas. The working gas stiffness has a maximum value if the expansion and compression processes are adiabatic which is given by [21]:

$$k = \frac{\gamma p A^2}{V} \quad (14)$$

The stiffness has a minimum value if the expansion and compression processes are isothermal which is given by [21]:

$$k = \frac{p A^2}{V} \quad (15)$$

Since the expansion and compression processes are polytropic then the working gas stiffness can be written as:

$$k = \frac{n p A^2}{V} \quad (16)$$

where n is the polytropic index which can be calculated from [38] as:

$$n = -\frac{V}{p}\frac{dp}{dv} \quad (17)$$

Applying the mass balance equation on the engine 3 control volume yields in [30]

$$m = m_e + m_c + m_r \quad (18)$$

Deriving the mass balance equation gives

$$\dot{m} = \dot{m}_e + \dot{m}_c + \dot{m}_r \quad (19)$$

The mass leakage in this engine is the summation of the leakage on the hot and cold pistons and is written as

$$\dot{m} = \dot{m}_{le} + \dot{m}_{lc} \quad (20)$$

The energy balance equation of the expansion volume can be written by considering the gas leakage at the expansion piston as follows

$$\dot{Q}_e + \dot{H}_e + c_p \dot{m}_e T_{re} = p\dot{v}_e + c_v(\dot{m_e} T_e) \quad (21)$$

By rearranging equation 21, the mass flow rate in the expansion chamber results in

$$\dot{m}_e = \frac{\frac{p\dot{v}_e}{R} + \frac{v_e \dot{p}}{\gamma R} - \frac{\dot{Q}_e + \dot{H}_e}{c_p}}{T_{re}} \quad (22)$$

Similarly, the mass flow rate in the compression chamber is written as

$$\dot{m}_c = \frac{\frac{p\dot{v}_c}{R} + \frac{v_c \dot{p}}{\gamma R} - \frac{\dot{Q}_c + \dot{H}_c}{c_p}}{T_{cr}} \quad (23)$$

The regenerator mass flow rate is calculated from

$$\dot{m}_r = \frac{V_r}{R T_r} \dot{p} \quad (24)$$

The differential form of the pressure obtained by combining Equations 19, 22, 23 and 24 becomes

$$\dot{p} = \frac{-p\left(\frac{\dot{v}_e}{T_{re}} + \frac{\dot{v}_c}{T_{cr}}\right) + \frac{R}{c_p}\left(\frac{\dot{Q}_e + \dot{H}_e}{T_{re}} + \frac{\dot{Q}_c + \dot{H}_c}{T_{cr}}\right) + R\dot{m}}{\frac{v_e}{\gamma T_{re}} + \frac{V_r}{T_r} + \frac{v_c}{\gamma T_{cr}}} \quad (25)$$

where v , T, $\dot{Q}, \dot{H}$ and m denote the volume, temperature, heat flow rate, enthalpy and mass leakage in the working spaces, respectively and subscripts e, r and c indicate the expansion, regeneration and compression space, respectively.

The Franchot engine enjoys small enthalpy loss as the leaks shuttle between similar temperature chambers. The enthalpy is calculated as [39]

$$\dot{H} = c_p \dot{m}_l T \quad (26)$$

where T depends on the mass leakage direction between opposite expansion or compression spaces. It is the source temperature for positive mass flow rate and working space temperature for negative mass flow rate.

The mass leakage through a clearance seal where the flow is laminar is calculated from [7][39]

$$\dot{m}_l = \pi D \frac{p + \dot{p}}{4RT_g}\left(\dot{x}\delta - \frac{\delta^3}{6\mu}\frac{p - \dot{p}}{L_g}\right) \quad (27)$$

where $p, \dot{p}, T_g, \dot{x}, \delta, \mu$ and L_g are instantaneous pressure, pressure at opposite chamber, gas temperature, linear piston velocity, piston to cylinder wall gap, dynamic viscosity and gab length.

Regenerator end temperatures are calculated from [30]:

$$T_{rh} = \frac{-\oint i\dot{m}_e T_e}{\oint (1-i)\dot{m}_e} \quad (28)$$

$$T_{rk} = \frac{-\oint j\dot{m}_c T_c}{\oint (1-j)\dot{m}_c} \quad (29)$$

where the parameters i and j are given by

$$i = \begin{cases} 1, & \dot{m}_e < 0 \\ 0, & \dot{m}_e \geq 0 \end{cases} \quad (30)$$

$$j = \begin{cases} 1, & \dot{m}_c < 0 \\ 0, & \dot{m}_c \geq 0 \end{cases} \quad (31)$$

Hence, the average regenerator temperature is:

$$T_r = \frac{T_{rh} - T_{rk}}{\ln \frac{T_{rh}}{T_{rk}}} \quad (32)$$

External irreversibility is considered through the heat addition and removal which are calculated from Newton's law of cooling [40]:

$$\dot{Q} = hA\Delta T \quad (33)$$

where h is the convective heat transfer coefficient, which holds for Reynolds' numbers between 1000 and 100,000 and is calculated as [41]:

$$h_e = 0.042 {D_h}^{-0.42} v^{0.58} p^{0.58} T^{-0.19}$$
$$h_c = 0.0236 {D_h}^{-0.47} v^{0.53} p^{0.53} T^{-0.11} \quad (34)$$

where $\Delta T, D_h, h_e \; and \; h_c$ are the temperature difference between the working gas and cylinder wall, hydraulic diameter, convective heat transfer during the expansion and compression, respectively.

4 Results and discussion

The model is implemented in Matlab/Simulink and solved using the Runga-Kutta method with a time step of 10^{-4}s. All results use the reference engine parameters listed in Table 2 unless otherwise stated. The reference engine is considered ideal and the mechanical Friction and regenerator pumping losses are considered as friction and damping load, respectively.

Table 2: Parameters of the reference engine

Name	*symbol*	*value/unit*
Stroke length	$\boldsymbol{L_e, L_c}$	*50 cm*
Bore diameter	$\boldsymbol{D_e, D_c}$	*2.5 cm*
Gas density	$\boldsymbol{\rho}$	*1.225 kg/m^3*
Reciprocator mass	$\boldsymbol{m}$	*0.1 kg*
Reg. volume	$\boldsymbol{V_r}$	*0 cm^3*
Number of phases	$\boldsymbol{n}$	*3*
Temperatures	$\boldsymbol{T_h, T_k}$	*450 K,300 K*
Link length	$\boldsymbol{y}$	*4 cm*
Working gas	*Air*	
Gas constant	$\boldsymbol{R}$	*287 J/kg.K*

4.1 Effect of friction

The start-up of the balanced compound engine is highly dependent on the static friction. Figure 5 shows the dynamic response of the 3-ph balanced compound Franchot engine in which, a minimum pressure difference of 3.67 kN/m^2 is needed to aid start-up. The force generated by this difference overcomes the static friction which is caused by the side forces and weight of the reciprocator. In a real application, pistons must be shifted from mid-stroke point so that a pressure difference can develop. Otherwise, an external starter might be required. However, it is very unlikely that all pistons stop exactly at the mid-stroke. The friction which is responsible for starting problems aids braking the balance at stopping stage especially when engine temperature difference is getting reduced. The mid-stroke equilibrium point may be affected by the difference in the regenerator volumes or the reduction of the swept volume due to the connecting rod. Unlike the balanced compound engine, the kinematic engine has the stroke, phase angle, phase shift and the instantaneous position of pistons predefined. Hence, pressure variations occur once the engine is heated which cause the kinematic engine to start-up regardless of the crank angle.

The dynamic response shows that the volume and phase angles are exactly 120^o degree. Different angles are less likely to happen due to the anticipated negative power which hinders the piston motion. At the steady state, piston displacements are symmetric and can be represented by sinusoidal functions [27].

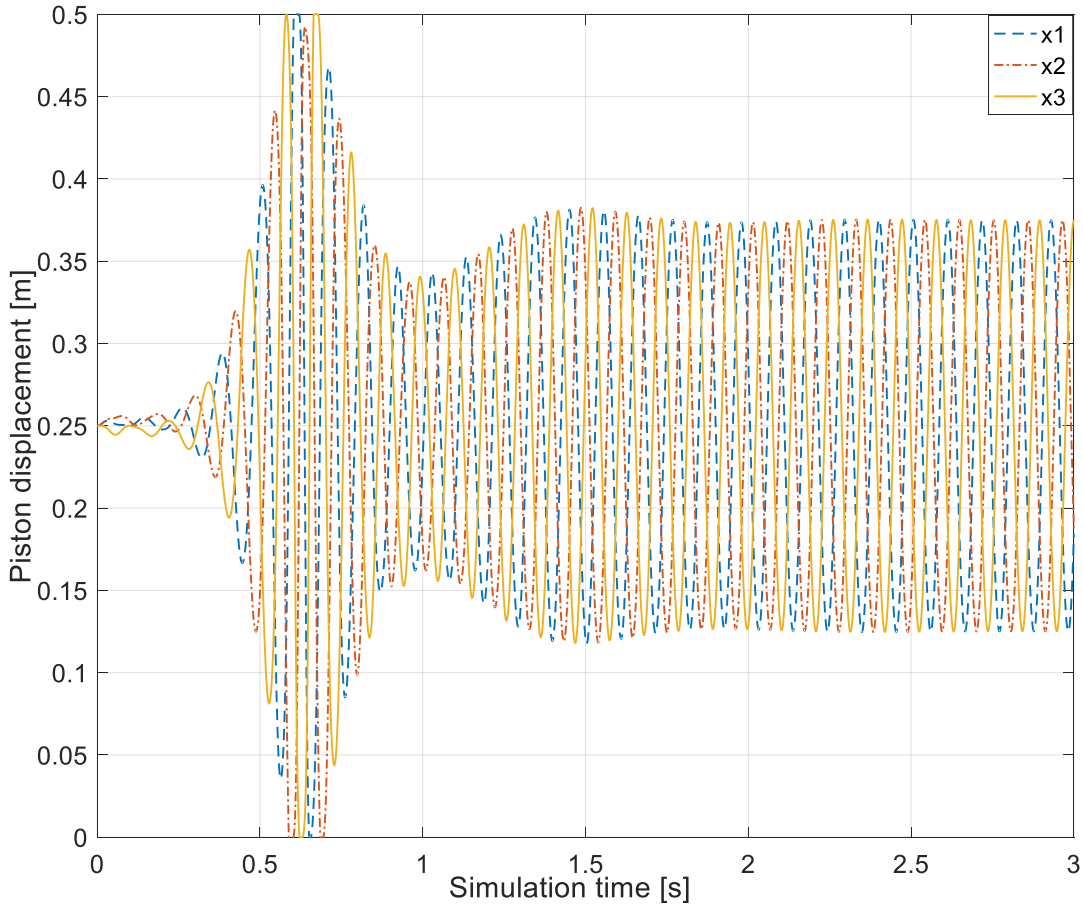

Figure 5: No-load dynamic start-up response of the reference 3-ph Franchot engine considering the mechanical friction.

The driving force and the side force due to the eccentricity of the new cranking mechanism are shown in Figure 6. The maximum driving force occurs at the full stroke while the side forces are minimum

hence maximum acceleration occurs. The worst case occurs around mid-stroke where the largest side forces and smallest driving force exist. However, at mid-stroke the kinetic energy is maximum and acts similar to the flywheel to overcome negative loads such as friction or speed dependant loads.

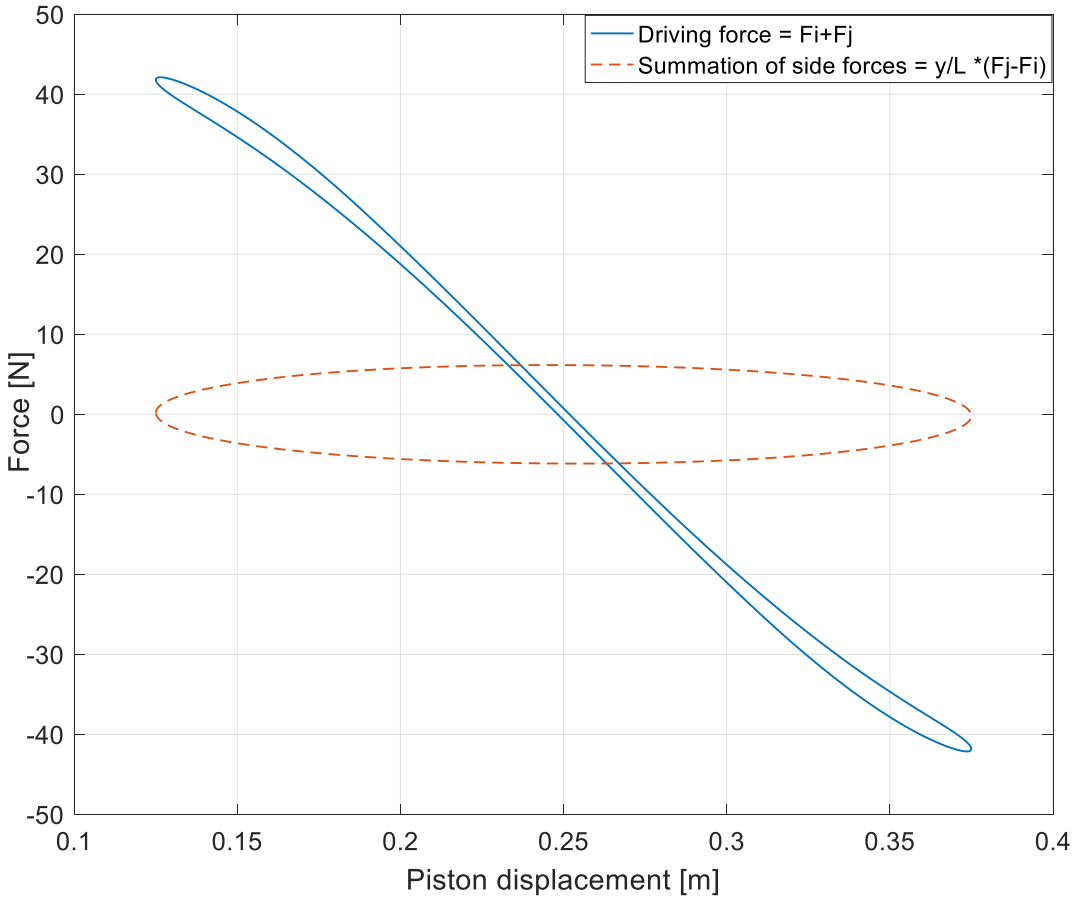

Figure 6: Loading forces of the new cranking mechanism.

4.2 Effect of gas leakage

In Stirling engines, gas leakage must be prevented in order to achieve the design performance. Different methods are used to overcome gas leakage such as using pressurised crankcase, tight seals, diaphragm pistons, liquid pistons and gas compensation. In this study, tight clearance seals are being suggested. The gas leakage due to the clearance of the connecting rod is not considered due to the small annular flow area and working pressure. In general, the gas leakage across pistons is small due to small diameters and low pressure variation [30]. The effect of gas leakage due to a typical radial clearance of $25\mu m$ [18] between the piston and cylinder wall is considered in Figure 7 for changing piston length. The gas leakage has almost no effect on the engine operation for piston lengths above 3cm. However, for smaller clearance piston lengths the engine stroke decreases as a response to increasing gas leakage while the engine frequency is only slightly affected. Hence, we suggest no mechanical springs or special gas prevention techniques to be used. For large gas leakage, even the kinematic engine will stall and contact seals are recommended for engines with high gas leakage.

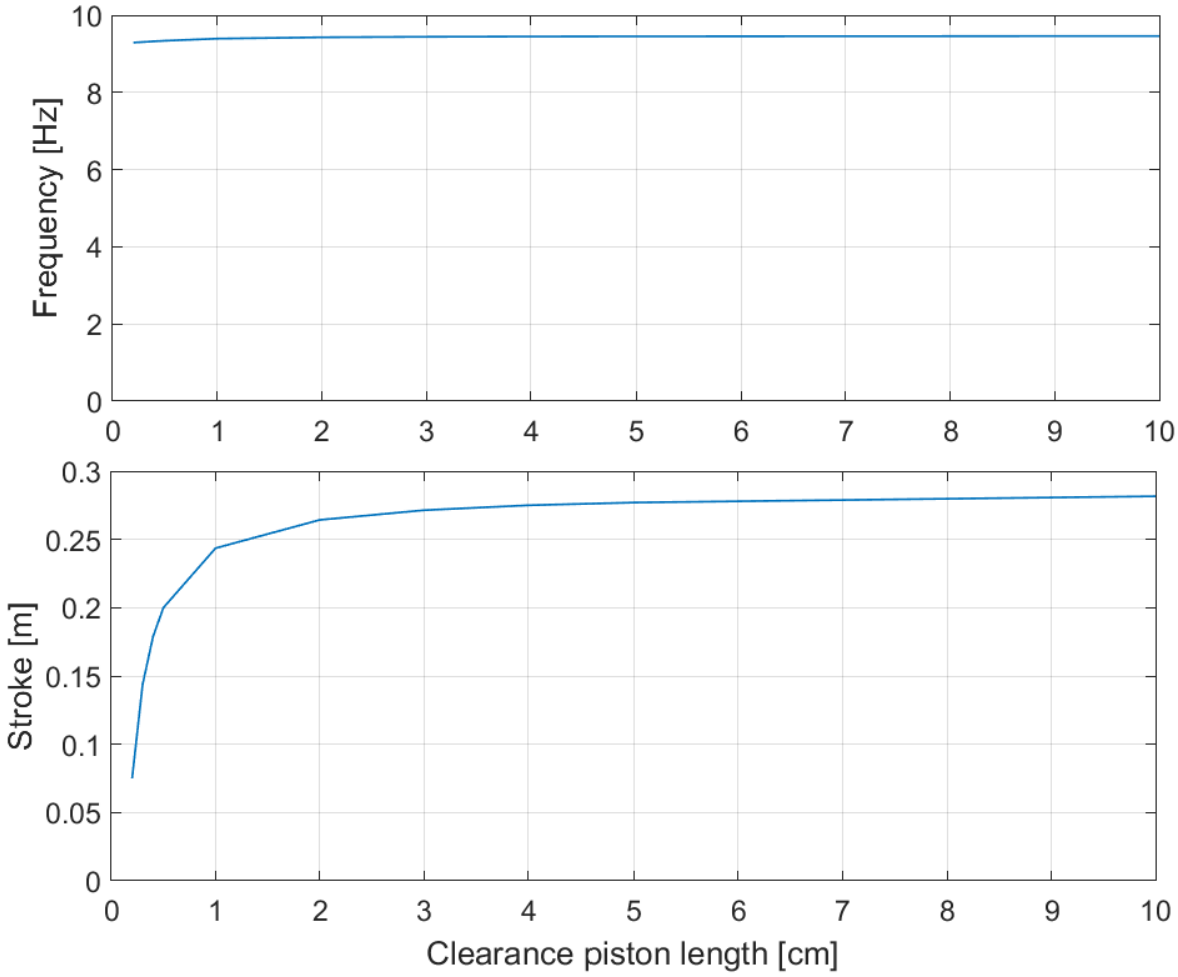

Figure 7: Steady state response of the reference engine with changing clearance piston length L_g at no-load condition.

4.3 Loading the balanced compound engine

In the kinematic engine, the engine stroke and piston instantaneous location are predetermined. Hence, the engine varies its speed as a response to the load. At no-load, the kinematic engine will accelerate until engine losses match the power generated and thus, the brake power is zero and engine speed is maximum. Loading the kinematic engine decreases its speed as well as the speed-accompanied losses. In contrast, the balanced compound engine has its speed determined by the stiffness of the gas spring and the reciprocator mass while its stroke is undetermined.

Figure 8 shows the effect of loading the 3-ph balanced compound engine by increasing the damping coefficient. The balanced compound Franchot engine has a slight frequency drop but a considerable stroke decrease as a response to increasing the load. Which make it suitable for fixed frequency applications like electricity generation. At no-load, the pistons reciprocate at the maximum stroke allowing heat to be transferred from the hot space to the cold space at highest rate without generating any useful power. At high engine loads, a stall point might be reached where no motion exists. Consequently, no heat will be exchanged and no power will be generated. Hence, a power maximum can be found in a point between the no-load and stall points while the efficiency is maximised as the load increases towards the stall point. The maximum power can be further maximised so that the stroke is slightly smaller than cylinder length but running the engine at no-load will cause the pistons to hit the walls. Hence, it is highly recommended that the engine must be designed at the no-load

condition unless the engine is always loaded. The phase angle is unaffected by the dynamic load and the engine is self-starting for various load values.

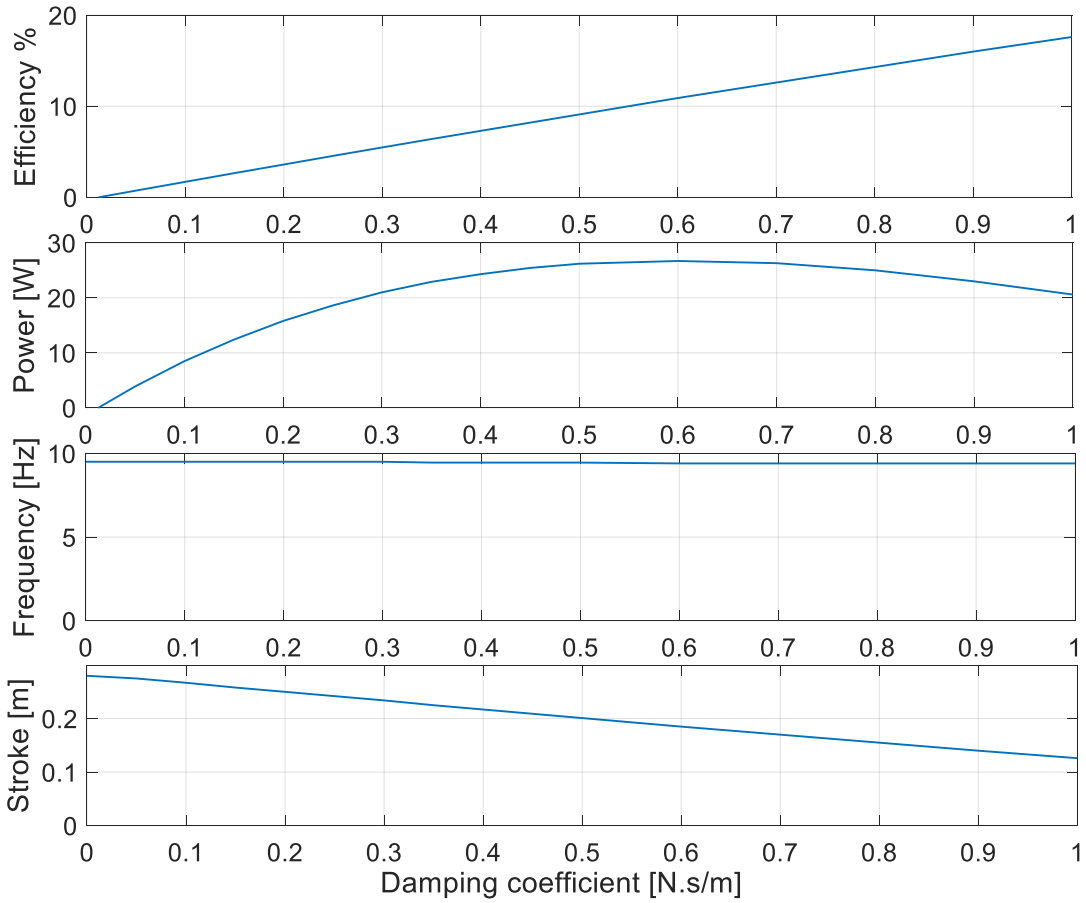

Figure 8: Steady state response of the reference engine for changing the damping load.

Figure 9 shows the PV diagram of the 3-ph balanced compound engine at the no-load, medium power and maximum power conditions. At the no-load condition, a butterfly shaped PV diagram shows two negative power regions where the compression overlaps with the expansion process and hence behaves like a gas spring [42]. This spring is important to the balanced compound engine to prevent the pistons from hitting the cylinder head by making gas cushions but it decreases the indicated work to zero at no-load. At medium and maximum powers, no negative work is found and both the pressure variation and swept volume are smaller than at the no-load case.

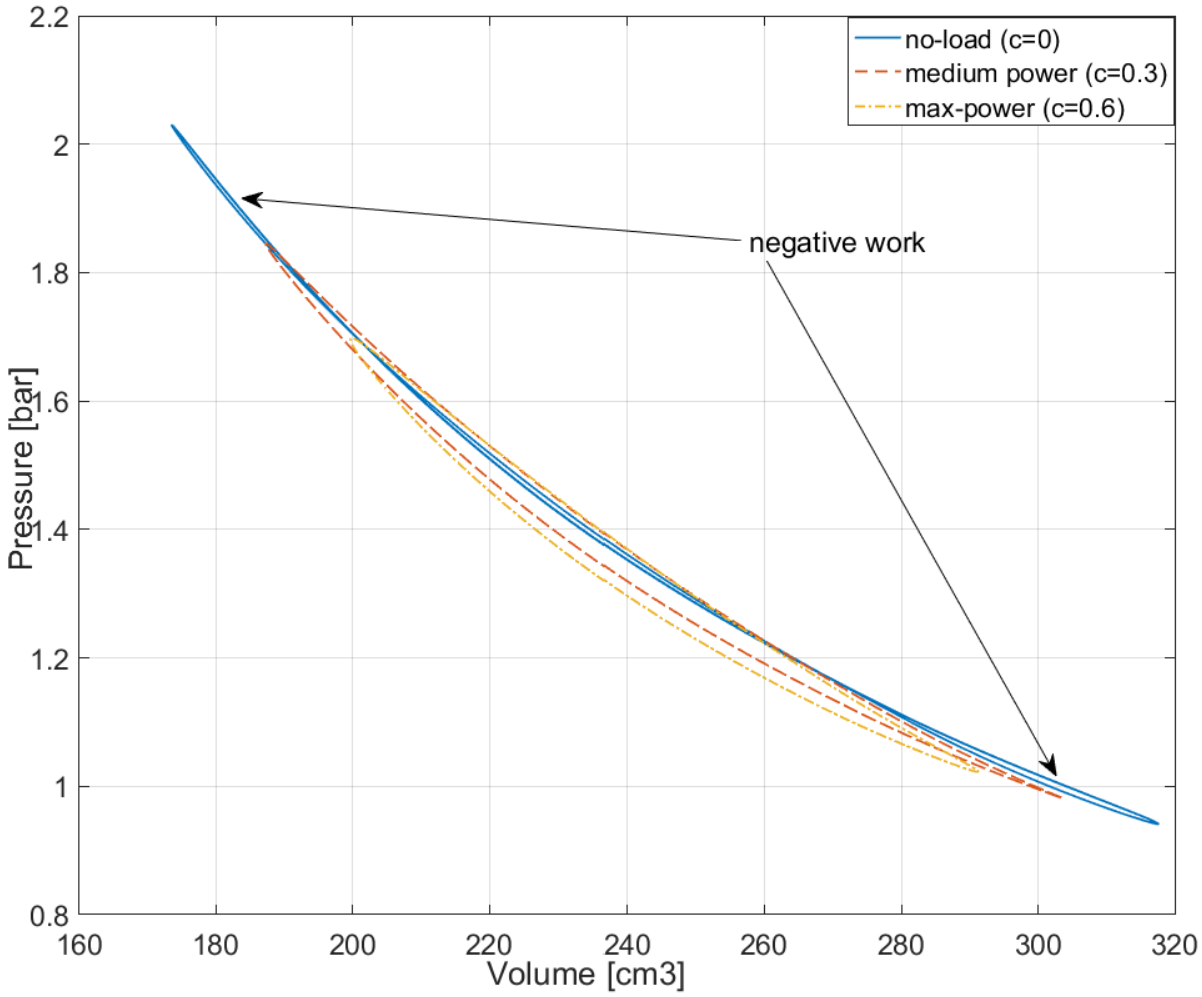

Figure 9: PV diagram of the balanced compound engine at no-load and maximum power conditions.

4.4 Effect of geometry

The geometry determines the resonant frequency, swept volume, heat transfer and piston forces which all contribute in the performance of the balanced compound engine with heated and cooled cylinders. The effect of increasing the engine cylinder diameters and lengths on the stroke and frequency of the unloaded engine are shown in Figure 10. The increase in the diameter results in a linear increase of the resonant frequency. Thus, a reduction of the engine stroke can be seen due to the increase in the piston area so that the positive engine power matches with the negative power.

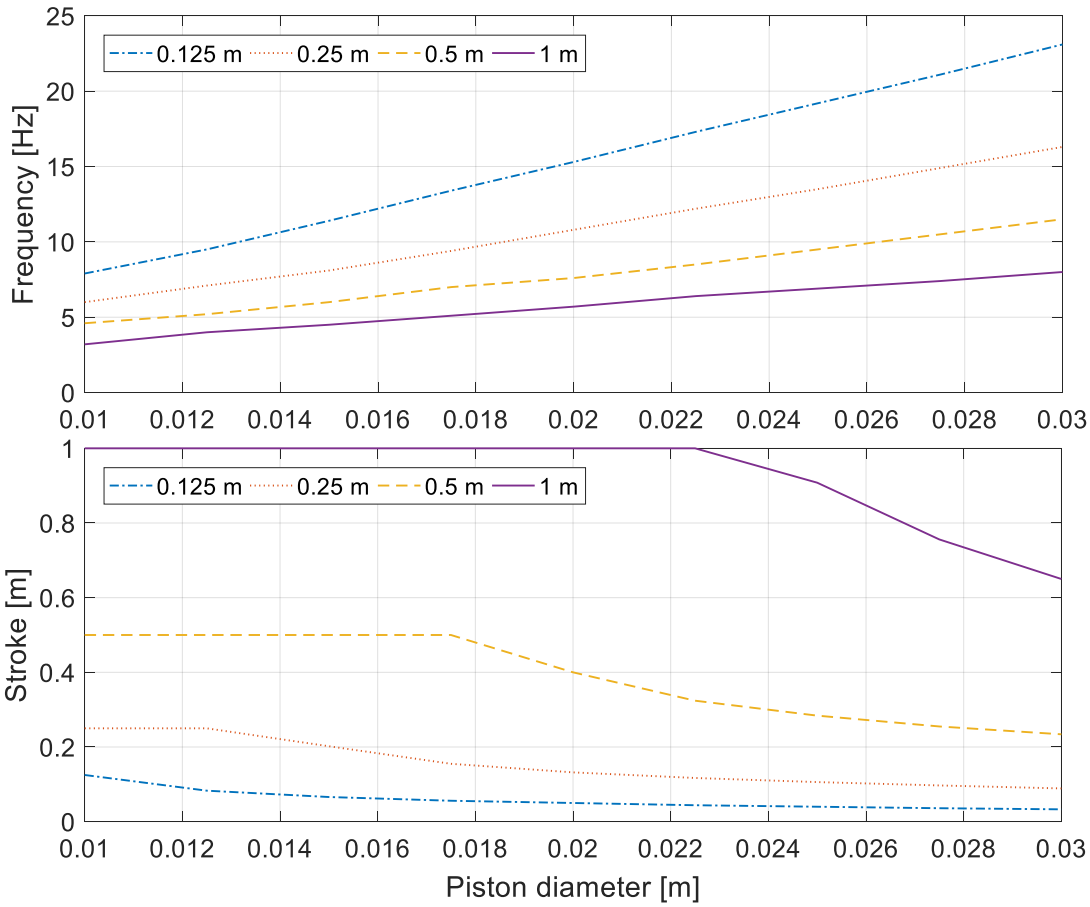

Figure 10: Steady state response of the reference engine for changing engine diameter at no-load and for various cylinder lengths (0.125, 0.25, 0.5 and 1m).

For long cylinders, the resonant frequency decreases as a result of reducing the working gas stiffness. In addition, longer cylinders also increase the heat transfer which in turn leads to longer strokes. It is found that the phase angle is kept unchanged with changing the cylinder geometry and the engine self-starts at no-load.

Figure 11 shows the influence of changing the diameter on the engine performance at the maximum power condition. It is found that increasing the diameter increases the maximum power and efficiency. The heat transfer increases due to increasing the Reynolds' number inside the engine cylinders which increases due to the diameter and the frequency of oscillation. The engine regulates itself by decreasing the stroke until maximising the power as a response to increasing the diameter.

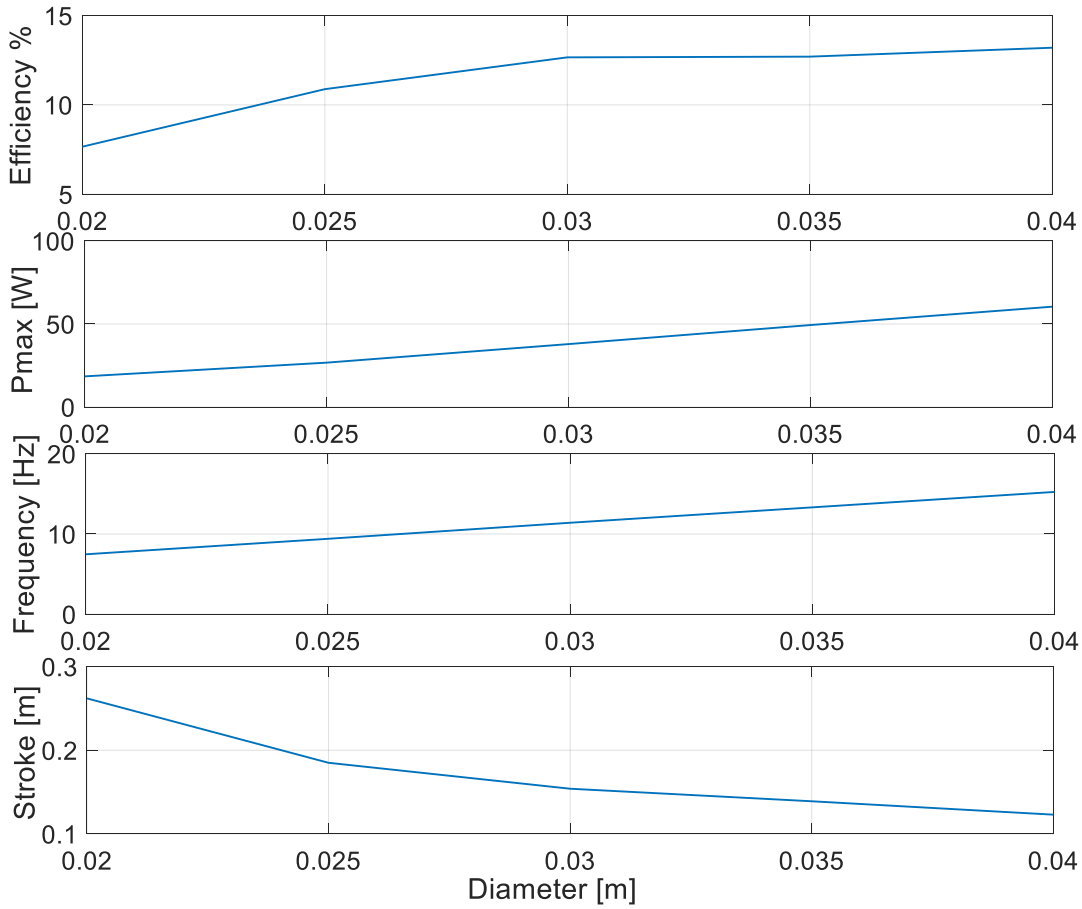

Figure 11: Performance of the balanced compound Franchot engine at the maximum power with changing piston diameter.

Large diameters generate large forces which help to overcome potential static mechanical frictions and loads hence ease the start-up of the balanced compound Franchot engine. Moreover, they prevent the pistons from hitting the cylinder especially at no-load condition.

4.5 Effect of temperature

The heat source temperature is the easiest parameter to control in the balanced compound engine and it has a major effect on engine power and efficiency. High temperature differences induce high-pressure variations and generate more cycle work than low temperatures. Thus both the frequency and stroke increase with increasing temperature differences as shown in Figure 12. The increase in the frequency can be attributed to the increase in the stiffness which is in turn increased as a response to the increased pressure variation. The phase angle is kept constant for changes in the temperature and the engine is self-staring for dynamic load. However, high temperature might cause the piston to hit the cylinder end plates. Hence, large temperatures require large diameters to decrease the stroke but this will also increase the frequency (see Figure 10). Alternatively, the engine load can be increased which will reduce the stroke without affecting the frequency and thus can prevent the piston hitting the cylinder end plates (see Figure 8). Accordingly, increasing the temperature can be used during the start-up to overcome the static friction.

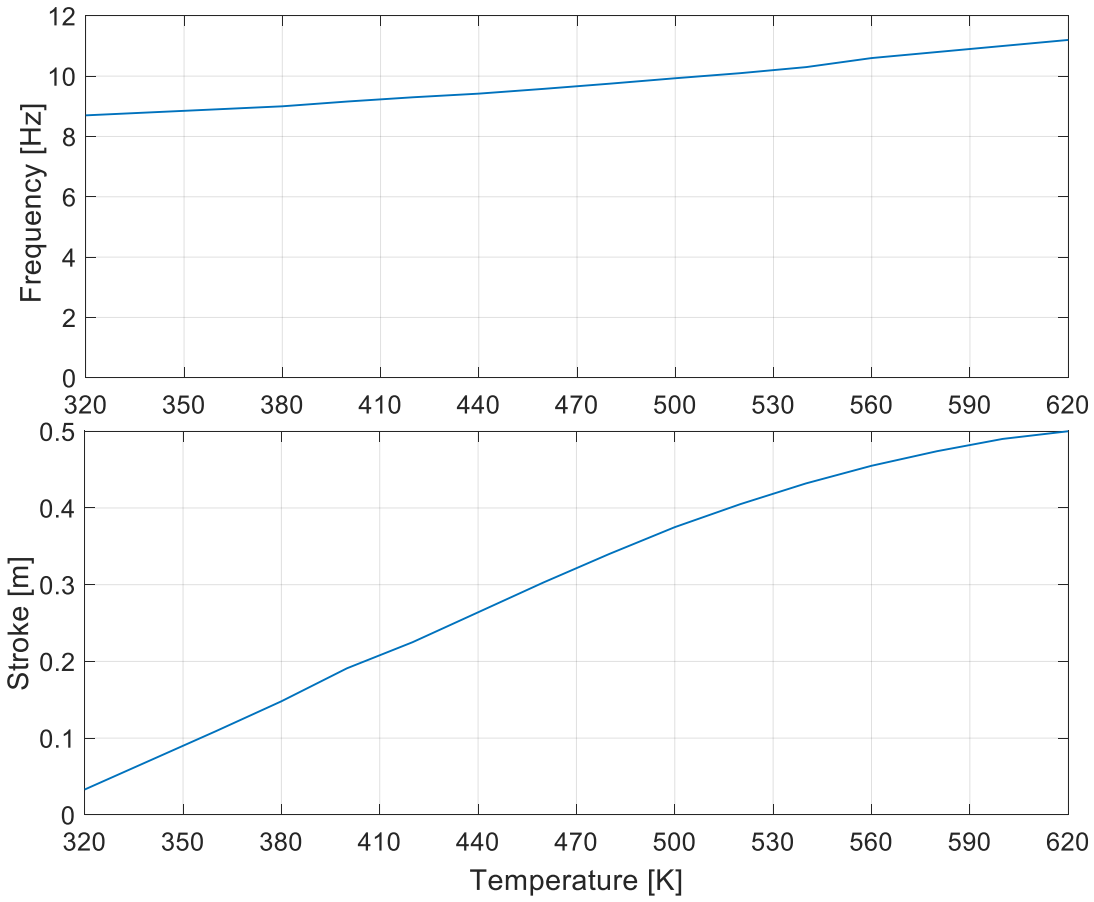

Figure 12: Steady state response of the reference engine for changing hot cylinder temperatures and at no-load condition.

4.6 Effect of regenerator dead volume

The dead volume increases the total engine volume, which reduces the gas stiffness and engine frequency. Moreover, an increased dead volume increases the engine thermal efficiency hence the engine stroke can increase. Thus, an increase in the stroke and decrease in the frequency is obtained for increasing the regenerator dead volume which can be seen in Figure 13.

At start-up, a large regenerator dead volume could prevent the pistons from moving due to the small pressure variation especially near the equilibrium point. Moreover, a large regenerator requires a long time to create a temperature gradient. Hence, an external kick-start or appropriate piston positioning might be required to start the motion. In addition, the dead volume can lead to the piston hitting the cylinder end plates hence causing an unstable operation but it can be optimised to maximise the power or enhance the efficiency. However, the self-starting capability and fixed phase angle is obtained for the 3-ph engine at no-load and dynamic load conditions for different regenerator volumes.

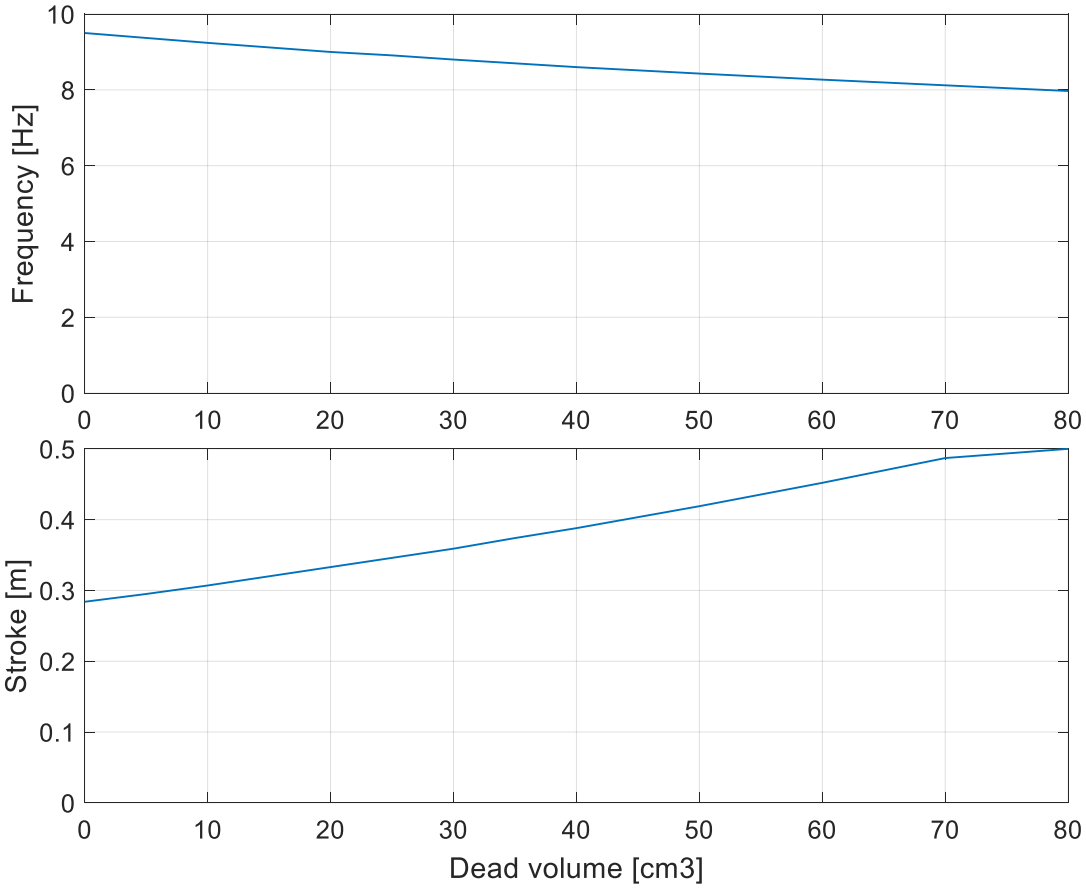

Figure 13: Steady state response of the reference engine for changing regenerator dead volumes and at no-load condition.

4.7 Effect of reciprocator mass

The mass should be as small as possible in ordered to have the lowest effect on the engine swept volumes, heat transfer and friction due to reciprocator weight. Reciprocating mass includes the pistons, connecting rods and the link between the connecting rods. Figure 14 shows that increasing the reciprocator mass causes the stroke to increase and frequency to decrease. Small masses increase the resonant frequency which behave similarly to increasing piston area. The self-starting capability and fixed phase angle is obtained for the 3-ph engine at the no-load condition with changing the mass of the reciprocator.

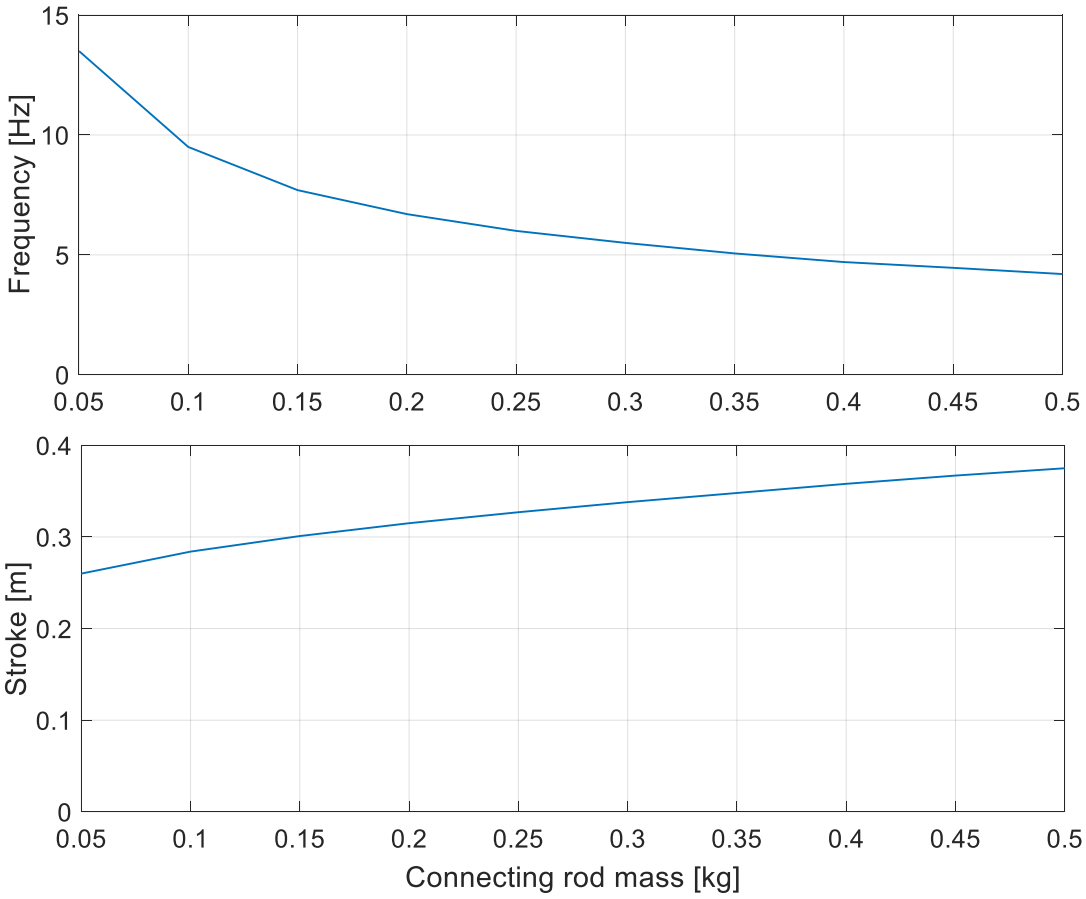

Figure 14: Steady state response of the reference engine for changing reciprocator masses and at no-load condition.

4.8 Effect of number of cylinders

The Franchot engine has the advantage of a flexible phase angle. For the balanced compound configuration, the phase angle is determined from the order of piston motion and regenerator connection. The number of cylinders is directly linked to the phase angle according to Table 1. The phase angle can be predicted for the 3-ph (six cylinders) and 4-ph (eight cylinders) Franchot engine since they have only single phase angles 120° and 90° respectively. In $n - ph$ Franchot engines where n is larger than four, the phase angle can take several values in the kinematic engine.

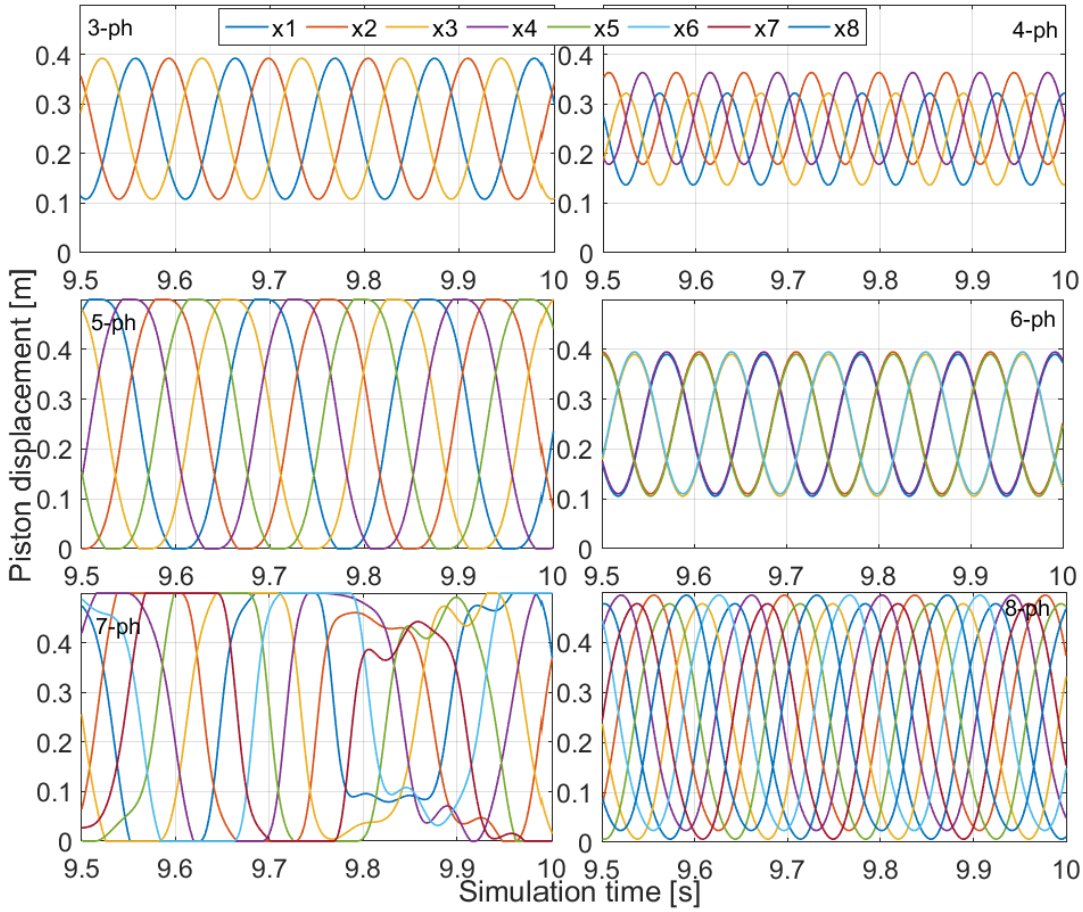

Figure 15: No-load quasi steady state response for three to eight phase Franchot engine. The reciprocators' motion is given according to the displacement notation.

Figure 15 shows that the $n-ph$ balanced compound Franchot engine always work on a single phase angle unlike the kinematic engine. The phase angle is determined from the lagging of a cold working volume of cylinder x_{i+1} to the neighbouring hot cylinder x_i because the regenerator connections are fixed. Hence, the motion sequence of the pistons in corresponding cylinders is used. Due to the even distribution of curves, the phase shift in a cycle is determined by dividing 360 by the number of distinguished phases. Following from this, the phase angle is calculated based on the number of phase shift peaks between the advancing and lagging curves $x_i \; and \; x_{i+1}$, respectively. For example, the $5-ph$ engine has a phase shift of 72° due five phases and each cold space x_{i+1} lags the corresponding hot space x_i by two peaks which equals 144°. The 6-ph engine has only three distinguished phases which result in a phase shift of 60° and hence a phase angle of 120° due to only two peaks. Although small phase angles where anticipated for engines with large number of cylinders [20] the balanced compound Franchot engine operates always at the largest possible phase angle. At this phase angle, the pistons encounter the smallest possible piston forces due to the lower pressure difference compared to smaller phase angles. This means the balanced compound Franchot engine prefers the least resisting phase angle among the ones listed in Table 1. Thus, the phase angle of the balanced compound $n-ph$ Franchot engine can be written as:

$$\theta = \begin{Bmatrix} 180 - \frac{180}{n} & for\ odd\ n \\ 180 - \frac{360}{n} & for\ even\ n \end{Bmatrix} \qquad 35$$

The 4-ph Franchot engine has the smallest possible phase angle of 90^o degree. This engine has the shortest stroke and largest frequency because a small phase angle increases the pressure variation which in turn increases the stiffness. Accordingly, the smallest frequency and the longest stroke can be found at the largest phase angle where hitting the cylinder might occur. The 3-ph and 6-ph Franchot engines have different number of cylinders but have nearly the same dynamic response due to having the same phase angle. Large phase angle such as in the 7-ph engine have unsteady response. Due to the large durations of hitting the wall, other pistons reciprocate creating pressure variations. However, the impact with the wall consumes all the piston kinematic energy. Hence, hitting the wall must be avoided for the engine longevity, durability, quietness and efficiency.

The odd phase balanced compound Franchot engines have similar phase angles and number of cylinders to the multi-cylinder Siemens configuration but different phase shifts as two pistons are moving together at the same time. The phase angle of the even phase Franchot engines lags behind odd phase engines as the number of cylinders increases. The smallest possible number of cylinders is 3, 4 and 6 in the Siemens configuration, Finkelstein arrangement and balanced compound Franchot engine, respectively.

5 Conclusion

The balanced compounding of the directly heated and cooled Franchot engine is mathematically modelled and the engine response with respect to changes in friction, load, geometry, temperature, dead volume and reciprocating mass has been discussed. The novel Franchot engine has a favourable phase angle of 120^o and short regenerator connections compared to the Finkelstein configuration. The friction created by side forces can be decreased by increasing the length of the engine and by decreasing the offset between the cylinders. The engine is self-starting because the friction prevents the engine from stopping exactly at mid stroke. Thus, the engine has great potential as a prime mover for liquid or heat pumps or electric generators.

Due to the absence of the crankshaft, the balanced compound Franchot engine can have incomplete strokes but with a fixed phase angle and nearly constant frequency as a response to increasing load. The performance of the free piston engine depends on the geometry, temperatures, dead volume, reciprocator mass, number of cylinders and load. Small loads, high temperatures, large dead volumes and low diameters increase the stroke which might lead to the pistons hitting the cylinder heads.

The dynamic model of the balanced compound Franchot engine confirms the potential phase angles that were found using the instantaneous power method for the 3-ph and 4-ph Franchot engines which equals the phase shift. In addition, it is shown that the $n - ph$ balanced compound Franchot engine always prefers the largest possible phase angle so that it operates with the least resisting loads.

In the balanced compounding, the Franchot engine can have only a single phase angle which limits its advantages. However, the phase angle can be adjusted by changing the number of cylinders. The simplest form of the $n - ph$ free piston engine is the 3-ph engine. It has the shortest regenerator connections, smallest number of cylinders, a favourable phase angle and it has potential for electricity generation. In contrast to the Finkelstein configuration, the side-by-side balanced compound 3-ph engine has a 120^o phase angle, shorter regenerator connections and long engine strokes but it could not eliminate the side forces on the connecting rods. The balanced compound engine is suggested for pumping and power generation applications as its response has nearly constant frequency with the load.

Acknowledgement

The authors would like to thank the British Council - HESPAL for the Ph.D scholarship for Jafar M. Daoud.

References

[1] G. Walker, "Coal-fired Stirling engines for railway locomotive and stationary power applications," *Proc Instn Mech Engrs*, vol. 197A, no. October, pp. 233–246, 1983.

[2] M. H. Ahmadi, H. Sayyaadi, S. Dehghani, and H. Hosseinzade, "Designing a solar powered Stirling heat engine based on multiple criteria: Maximized thermal efficiency and power," *Energy Convers. Manag.*, vol. 75, pp. 282–291, Nov. 2013.

[3] S. Toghyani, A. Kasaeian, and M. H. Ahmadi, "Multi-objective optimization of Stirling engine using non-ideal adiabatic method," *Energy Convers. Manag.*, vol. 80, pp. 54–62, Apr. 2014.

[4] M. H. Ahmadi, M. A. Ahmadi, A. Mellit, F. Pourfayaz, and M. Feidt, "Thermodynamic analysis and multi objective optimization of performance of solar dish Stirling engine by the centrality of entransy and entropy generation," *Int. J. Electr. Power Energy Syst.*, vol. 78, pp. 88–95, Jun. 2016.

[5] B. Hoegel, D. Pons, M. Gschwendtner, and A. Tucker, "Theoretical investigation of the performance of an Alpha Stirling engine for low temperature applications," *ISEC Int. Stirling Engine Comm.*, no. January, 2012.

[6] T. Finkelstein, "Optimization of phase angle and volume ratio for Stirling engines," Jan. 1960.

[7] M. H. Ahmadi, M.-A. Ahmadi, and F. Pourfayaz, "Thermal models for analysis of performance of Stirling engine: A review," *Renew. Sustain. Energy Rev.*, vol. 68, no. October 2016, pp. 168–184, 2017.

[8] N. W. Lane and W. T. Beale, "Free-piston Stirling design features," *Eighth International Stirling Engine Conference*. 1997.

[9] G. Fenies, F. Formosa, J. Ramousse, and A. Badel, "Double acting Stirling engine: Modeling, experiments and optimization," *Appl. Energy*, vol. 159, pp. 350–361, 2015.

[10] E. D. Rogdakis, N. A. Bormpilas, and I. K. Koniakos, "A thermodynamic study for the optimization of stable operation of free piston Stirling engines," *Energy Convers. Manag.*, vol. 45, no. 4, pp. 575–593, 2004.

[11] W. T. Beale, "Free Piston Stirling Engines - Some Model Tests and Simulations," 1969, pp. 1–10.

[12] W. T. BEALE, "Stirling cycle type thermal device," U.S. Patent 3,552,120, 1971.

[13] A. Der Minassians and S. R. Sanders, "Multiphase Stirling Engines," *J. Sol. Energy Eng.*, vol. 131, no. 2, p. 21013, 2009.

[14] G. Walker and J. R. Senft, *Free Piston Stirling Engines*, First edit., vol. 12. Berlin, Heidelberg: Springer Berlin Heidelberg, 1985.

[15] M. A. White, J. E. Augenblick, and A. A. Peterson, "Double acting thermodynamically resonant free-piston multicylinder Stirling system and method," U.S. Patent 7,134,279 B2, 2006.

[16] W. T. Beale, "Pressure modulation system for load matching and stroke limitation of Stirling cycle apparatus," U.S. Patent 4,458,495, 1984.

[17] D. G. Thombare and S. K. Verma, "Technological development in the Stirling cycle engines," *Renew. Sustain. Energy Rev.*, vol. 12, no. 1, pp. 1–38, Jan. 2008.

[18] B. Hoegel, “Thermodynamics-based design of stirling engines for low-temperature heat sources.,” University of Canterbury, 2014.

[19] D. M. Berchowitz and Y.-R. Kwon, “Multiple Cylinder Free-Piston Stirling Machinery,” *J. Power Energy Syst.*, vol. 2, no. 5, pp. 1209–1220, 2008.

[20] D. M. Berchowitz and Y.-R. KWon, “Multiple-cylinder, free-piston, alpha configured Stirling engines and heat pumps with stepped pistons,” U.S. Patent 7,171,811 B1, 2007.

[21] A. Der Minassians, “Stirling Engines for Low-Temperature Solar-Thermal- Electric Power Generation,” University of California at Berkeley, 2007.

[22] C. D. West, “Liquid-piston Stirling machines,” in *2nd International Conference on Stirling engines*, 1984, pp. 15–36.

[23] J. W. Mason and J. W. Stevens, “Characterization of a solar-powered fluidyne test bed,” *Sustain. Energy Technol. Assessments*, vol. 8, pp. 1–8, 2014.

[24] T. Finkelstein, “balanced compounding of Stirling machines,” in *Intersociety Energy Conversion Engineering Conference,13th*, 1978, pp. 1791–1797.

[25] T. Finkelstein, “Method and device for balanced compounding of Stirling cycle machines,” U.S. Patent 4,199,945, 1980.

[26] T. Finkelstein, “Analysis of Heat-Activated Stirling Heat Pump,” in *Intersociety Energy Conversion Engineering Conference*, 1980, pp. 1788–1796.

[27] T. Finkelstein, “Isothermal Sinusoidal Analysis of Balanced Compound Vuilleumier Heat Pumps,” in *27th Intersociety Energy Conversion Engineering Conference (1992)*, 1992.

[28] Robert F. McConaghy, “Multi-cylinder free piston Stirling engine,” U.S. Patent 0,193,266 A1, 2007.

[29] M. W. Dadd, “Linear Multi-cylinder Stirling Cycle Machine,” U.S. Patent 8,820,068 B2, 2014.

[30] J. M. Daoud and D. Friedrich, “Performance investigation of a novel Franchot engine design,” *Int. J. Energy Res.*, Aug. 2017.

[31] J. M. Daoud and D. Friedrich, “Parametric Study of an Air Charged Franchot Engine with Novel Hot and Cold Isothermalizers,” *Inventions*, vol. 2, no. 4, p. 35, Dec. 2017.

[32] J. M. Daoud and D. Friedrich, “A novel Franchot engine design based on the balanced compounding method,” *J. Mech. Sci. Technol.*, vol. under revi.

[33] S. Chatterton and P. Pennacchi, “Design of a Novel Multicylinder Stirling Engine,” *J. Mech. Des.*, vol. 137, no. 4, p. 42303, 2015.

[34] H. Karabulut, “Dynamic analysis of a free piston Stirling engine working with closed and open thermodynamic cycles,” *Renew. Energy*, vol. 36, no. 6, pp. 1704–1709, 2011.

[35] R. W. Redlich and D. M. Berchowitz, “Linear Dynamics of Free-Piston Stirling Engines,” *Proc. Inst. Mech. Eng. Part A Power Process Eng.*, vol. 199, no. 3, pp. 203–213, Aug. 1985.

[36] K. Hirata, “A10 Development of 2-cylinder Double-Acting Stirling Engine,” in *The Proceedings of the Symposium on Stirlling Cycle*, 2006, vol. 2006.10, pp. 93–96.

[37] S.-Y. Kim and D. Berchowitz, “Specific Power Estimations for Free-Piston Stirling Engines,” in *4th International Energy Conversion Engineering Conference and Exhibit (IECEC)*, 2006, no. June.

[38] M. Babaelahi and H. Sayyaadi, “Modified PSVL: A second order model for thermal simulation of Stirling engines based on convective-polytropic heat transfer of working spaces,” *Appl. Therm. Eng.*, vol. 85, pp. 340–355, 2015.

[39] R. Li, L. Grosu, and D. Queiros-condé, “Losses effect on the performance of a Gamma type Stirling engine,” *Energy Convers. Manag.*, vol. 114, pp. 28–37, 2016.

[40] M. Costea and M. Feidt, “The effect of the overall heat transfer coefficient variation on the optimal distribution of the heat transfer surface conductance or area in a Stirling engine,” *Energy Convers. Manag.*, vol. 39, no. 16–18, pp. 1753–1761, Nov. 1998.

[41] F. Toda, S. Iwamoto, M. Matsuo, and Y. Umezane, “Heat Transfer on a Small Stirling Engine,” *J. Mar. Eng. Soc. JAPAN*, vol. 25, no. 6, pp. 358–365, 1990.

[42] C. Fernández-Aballí-Altamirano, M. Calcoen, E. Vandermeersch, and J. J. González-Bayón, “Experimental Tailer like Thermal Lag Engine to obtain pressure and volume diagrams,” *Ing. Mecánica*, vol. 16, no. 1, pp. 35–40, 2013.